Analysis of the expression and mechanism of follistatin-like protein 1 in cervical cancer

ZHEN LIU, HONG ZHANG and XIAOXIA HU

Department of Gynecology, The People's Hospital of Guangxi Zhuang Autonomous Region,
Guangxi Academy of Medical Sciences, Nanning, Guangxi Zhuang Autonomous Region 530021, P.R. China

Abstract. The abnormal expression of follistatin-like protein 1 (FSTL1) in various tumors is a crucial regulator of the biological process of tumorigenesis. Nonetheless, the regulatory role of FSTL1 in cervical cancer is yet to be elucidated. Hence, the present study aimed to explore the expression, function, and molecular mechanism of FSTL1 in cervical cancer. The expression of FSTL1 in normal and cervical cancer tissues was examined using quantitative reverse transcription-polymerase chain reaction and immuno-histochemistry assays. The effects of abnormal expression of FSTL1 on cervical cancer cells were assessed using colony formation, MTT, wound-healing, Transwell, apoptosis, and nude mouse tumorigenicity assays. FSTL1-related molecular mechanisms were screened using gene chip analysis. Western blotting analysis was used to verify the regulatory mechanisms of FSTL1 in cervical cancer. The results indicated that the expression of FSTL1 was downregulated in cervical cancer tissues and that its downregulation was associated with tumor differentiation, pathologic type, and infiltration depth. Moreover, FSTL1 inhibited the proliferation, migration, and invasion of cervical cancer cells as well as xenograft tumor growth and promoted cell apoptosis. In addition, the findings of gene chip analysis suggested that the differentially expressed genes of FSTL1 were predominantly enriched in multiple signaling pathways, of which the insulin-like growth factor (IGF)-1 signaling pathway was significantly activated. Western blotting suggested the involvement of FSTL1 in the regulation of the IGF-1R/PI3K/AKT/BCL-2 signaling pathway. These data establish the downregulation of FSTL1

in cervical cancer tissues. FSTL1 inhibited the proliferation, migration, and invasion of cervical cancer cells and promoted their apoptosis. Furthermore, xenograft tumor growth in nude mice was inhibited. FSTL1 may be involved in the regulation of the IGF-1R/PI3K/AKT/BCL-2 signaling pathway in cervical cancer. Therefore, FSTL1 may be employed as a novel biomarker to determine the extent of disease progression in patients with cervical cancer.

Introduction

Cervical cancer is one of the most common malignancies of the female reproductive system and seriously threatens the life and health of women. Approximately 570,000 new cases of cervical cancer are diagnosed annually, and ~311,000 patients succumb to the disease worldwide (1). Several investigations have indicated that the incidence of cervical cancer is closely related to human papillomavirus (HPV) infection (2,3). Owing to the continuous improvements in cervical cancer detection and diagnosis technologies and standardized HPV screening, the incidence of this disease has decreased in countries that have HPV screening and vaccination programs. The major issue with cervical cancer is the lack of such programs in low-income countries. Women in these countries require new therapies, which again are likely to be too expensive, but hopefully, a target can be identified. Therefore, developing novel diagnostic and therapeutic biomarkers to enhance the overall survival of patients with cervical cancer is the need of the hour.

Follistatin-like protein 1 (FSTL1), a type of secretory glycoprotein, is expressed in most mammalian cells, with the exception of peripheral lymphocytes. FSTL1 is localized on chromosome 3q13.33 and comprises 308 amino acids. The protein belongs to the secreted protein acidic and rich in cysteine (SPARC) family (4). However, the functions and biological characteristics of FSTL1 are different from those of other members of the SPARC family (5). In recent years, several studies have confirmed that FSTL1 functions as a crucial regulator in various biological processes and that it has a key effect on the occurrence and development of cancer. Epithelial ovarian cancer (6), non-small cell lung cancer (7), clear cell renal cell carcinoma (8), nasopharyngeal carcinoma (9), esophageal squamous cell carcinoma (10), gastric cancer (11), prostate cancer (12), and hepatocellular carcinoma are a few examples (13). FSTL1 plays a role in several

Correspondence to: Dr Xiaoxia Hu or Dr Hong Zhang, Department of Gynecology, The People's Hospital of Guangxi Zhuang Autonomous Region, Guangxi Academy of Medical Sciences, 6 Taoyuan Road, Nanning, Guangxi Zhuang Autonomous Region 530021, P.R. China
E-mail: huxxia@hotmail.com
E-mail: 270076755@qq.com

cancer-related signaling pathways. For example, the protein can retard the progression of clear cell renal cell carcinoma by inhibiting the NF-kB and HIF-2α signaling pathways (8). In hepatocellular carcinoma (13), FSTL1 promotes tumor growth by activating AKT via regulation of TLR4/CD14. With respect to cervical cancer, only one study has reported that FSTL1 could significantly inhibit the proliferation and invasion of cervical cancer cells through negative regulation of the BMP4/Smad1/5/9 signaling pathway (14). A previous study by the authors confirmed that FSTL1 is a direct target of miR-9, which is involved in the migration of cervical cancer cells (15). Nonetheless, clarity on the clinical significance and mechanism of FSTL1 is lacking in cervical cancer.

Hence, in the present study, the expression, function, and molecular mechanisms of FSTL1 in cervical cancer were investigated. The expression of FSTL1 in cervical tissues was examined. Subsequently, the effects of abnormal expression of FSTL1 on cervical cancer cells were assessed using *in vivo* animal experiments and functional *in vitro* experiments. Finally, the molecular mechanisms associated with FSTL1 were examined in HeLa and SiHa cells. The results indicated the downregulation of FSTL1 in cervical cancer tissues. FSTL1 inhibited the proliferation, migration, and invasion of cervical cancer cells and promoted their apoptosis. This protein is likely to be involved in the regulation of the IGF-1R/PI3K/AKT/BCL-2 signaling pathway in cervical cancer.

Materials and methods

Clinical samples and cell lines. A total of 117 cervical cancer tissues were collected from the People's Hospital of Guangxi Zhuang Autonomous Region (Nanning, China) between September 2012 and June 2017. The non-tumor tissues were composed of 29 tumor-adjacent tissues and 43 normal cervical tissues, including uterine prolapse (n=4), endometriosis (n=19), and hysteromyoma (n=20), which were collected during the same period. None of the patients received any treatment before the operation, as confirmed by pathologists after the operation. The clinical data of all patients with cervical cancer are shown in Table I. HeLa and SiHa cells were obtained from the Shanghai Cell Bank, Chinese Academy of Sciences. HeLa and SiHa cells were maintained in RPMI-1640 medium (Gibco; Thermo Fisher Scientific, Inc.) supplemented with 10% fetal cow serum (Gibco; Thermo Fisher Scientific, Inc.) supplemented with 1% penicillin and streptomycin at 37°C in a humidified atmosphere containing 5% CO_2. The present study complied with the guidelines outlined in the Declaration of Helsinki and was approved (approval no. KY-LW-2017-5) by the Ethics Committee of the People's Hospital of Guangxi Zhuang Autonomous Region (Nanning, China). Written informed consent was obtained from all patients.

RNA extraction and reverse transcription-quantitative PCR (RT-qPCR). Total RNA was extracted by using TRIzol® reagent (Invitrogen; Thermo Fisher Scientific, Inc.), and 500 ng of purified RNA was reverse transcribed into cDNA by using the Takara Reverse Transcription kit, following the manufacturer's instructions. RT-qPCR was performed by using the SYBR Green PCR Master Mix Kit on the ABI

7500 Real-Time PCR System (Applied Biosystems; Thermo Fisher Scientific, Inc.). Briefly, after an initial denaturation step at 95°C for 15 min, the amplifications were conducted with 40 cycles at a melting temperature of 95°C for 10 sec, followed by an annealing temperature of 60°C for 23 sec. GAPDH was selected as the housekeeping gene. The relative expression of FSTL1 was calculated by using the standard $2^{-\Delta\Delta Cq}$ method (16). The special primer sequences used were as follows: FSTL1 forward, 5'-GAGGGCAAGAGTACACCA-3' and reverse, 5'-TACGGCATAGACGACAGC-3'; GAPDH forward, 5'-CATGAGAAGTATGACAACAGCCT-3' and reverse, 5'-AGTCCTTCCACGATACCAAAG-3'. The FSTL1 mRNA expression was divided into high-expression and low-expression groups based on the median expression of FSTL1 mRNA.

Immunohistochemistry (IHC). The cervical tissues were fixed in 4% polyoxymethylene for 24 h at room temperature, embedded in paraffin and made into 3.5-μm thick sections. All cervical tissue sections were dewaxed and hydrated by an automatic dewaxing machine (ST5020; Leica Microsystems GmbH). The slides were treated under high pressure for antigen retrieval and 3% hydrogen peroxide to remove endogenous peroxidase. Subsequently, the sections were incubated with specific primary antibodies against FSTL1 (1:250; cat. no. ab71548; Abcam) at 4°C overnight. Known positive tissues (prostate cancer) were assigned to the positive-control group and phosphate-buffered saline (PBS) was used instead of the primary antibody in the negative-control group. The slides were then incubated with goat-anti-mouse/rabbit secondary antibodies (cat. no. PV-9000; OriGene Technologies, Inc.) at 37°C for 20 min, followed by staining by using the DAB detection kit (cat. no. ZLI9018; OriGene Technologies, Inc.). The slides were sequentially stained with hematoxylin, followed by differentiation in 0.5% hydrochloric acid alcohol, 1% ammonia water anti-blue, gradient alcohol dehydration, and neutral gum sealing. Finally, the slides were examined using a light microscope (BX51; Olympus Corporation). The proportion of stained cells was scored as follows: 0-25% (1), 25-50% (2), 50-75% (3), and 75-100% (4). The intensity of the stained cells was scored as follows: negative (0), weak (1), moderate (2) and strong (3). The final immunoreactivity score (IRS) was counted by summing the proportion and intensity scores (17). The IRS was finally confirmed by two independent pathologists from the People's Hospital of Guangxi Zhuang Autonomous Region. The FSTL1 expression at the protein level was classified as high expression or low expression group based on the median of IRS.

Hematoxylin-eosin (H&E) staining. All cervical tissue slides were dewaxed and hydrated in an automatic dewaxing machine (ST5020; Leica Microsystems GmbH), followed by rinsing in distilled water for 5 min and staining with hematoxylin. Next, the slides were immersed for differentiation in 0.5% hydrochloric acid alcohol and 1% ammonia water anti-blue for a few seconds. Subsequently, the slides were washed with distilled water for 5 min and then stained with 0.5% eosin for 2 min at room temperature. Finally, the slides were subjected to dehydration in a gradient series of alcohol and then sealed with neutral gum, followed by observation using a light microscope (BX51; Olympus Corporation).

Table I. Associations between FSTL1 expression and clinicopathological characteristics in cervical cancer patients.

Clinicopathological characteristics	Immunoreactivity score of FSTL1 protein expression				FSTL1 mRNA expression			
	Total cases (n=84)	Number of low cases (n=45)	Number of high cases (n=39)	P-value	Total cases (n=77)	Number of low cases (n=38)	Number of high cases (n=39)	P-value
Age				0.899				0.424
<50	36	19	17		39	21	18	
≥50	48	26	22		38	17	21	
Pathologic types				0.142				0.05
Squamous carcinomas	70	35	35		60	33	27	
Adenocarcinoma	14	10	4		15	4	11	
Other	-	-	-		2	1	1	
Degree of differentiation								
High	17	4	13		19	9	10	
Middle	49	26	23		32	17	15	
Low	18	15	3		26	12	14	
Maximum diameter (cm)				1				0.104
>4	10	5	5		20	13	7	
≤4	74	40	34		57	25	32	
FIGO stage				0.517				0.645
IA	-	-	-		4	3	1	
IB	61	34	27		44	20	24	
II	23	11	12		20	11	9	
≥III	-	-	-		9	4	5	
Infiltration depth[a]				0.021				0.037
>50	52	33	19		44	26	18	
≤50	32	12	20		33	12	22	
lymphatic metastasis				0.262				0.842
Negative	69	35	34		58	29	29	
Positive	15	10	5		19	9	10	
Vascular invasion				0.851				0.707
Negative	40	21	19		47	24	23	
Positive	44	24	20		30	14	16	
Nerve infiltration				1				0.665
Negative	77	41	36		70	34	36	
Positive	7	4	3		7	4	3	
Uterus and its attachments				0.491				0.564
Negative	44	22	22		55	26	29	
Positive	40	23	17		22	12	10	

'-' no relevant patient information; [a]Infiltration depth of tumor account for percentage of the whole cervical wall. FSTL1, follistatin-like protein 1.

Construction, infection, and screening of lentiviral overexpression (OE) of FSTL1. Lentiviral vector harboring FSTL1 was constructed and packaged by Shanghai GeneChem Co., Ltd. Briefly, cervical cancer cells (3-6x10⁴ cells/well) were seeded into six-well plates and cultured at 37˚C for 24 h under a humidified atmosphere of 5% CO_2. On the next day, the cells were infected with lentivirus-FSTL1-puro or lentivirus-negative control (NC)-puro [multiplicity of infection (MOI) was as follows: HeLa, $2x10^7$ TU/ml; SiHa: $1x10^7$ TU/ml] using polybrene or enhanced infection solution (Shanghai GeneChem Co., Ltd.). The culture medium was replaced after 12 h. Subsequently, puromycin (1.0 μg/ml) was added to the culture medium at 72 h after infection. The stable expression cell lines of FSTL1 were selected with puromycin

for 2 weeks. The FSTL1 expression at the mRNA and protein levels in cervical cancer cells was detected by RT-qPCR and western blotting, respectively.

Knockout (KO) of FSTL1 by using CRISPR/Cas9 technology. A total of three small-guide RNAs (sgRNAs) targeting FSTL1 were designed and used to construct CRISPR/CRISPR-associated (Cas)9-FSTL1 lentiviral particles. The three sgRNA-FSTL1 sequences were as follows: sgRNA-1(KO1): AGTGTCCATCGTAATCAACC; sgRNA-2(KO2): ACTTACCTCAATGCAGAGAC; and sgRNA3(KO3): GTAAGTCCATCTGCCAGCCC. Screening of biologically active sgRNA was performed by the Cruiser™ method. Cas9 and sgRNA lentiviral particles were constructed and packaged by Shanghai GeneChem Co., Ltd. Briefly, the cells (3-6x10⁴ cells/well) were seeded into six-well plates and cultured at 37°C for 24 h in a humidified atmosphere of 5% CO_2. On the next day, the cells were infected with lenti-cas9-puro lentiviral particles using polybrene or enhanced infection solution (Shanghai GeneChem Co., Ltd.). The culture medium was replaced after 12 h. Then, puromycin (1.2 µg/ml) was added to the culture medium at 72 h after infection. The stable expression cell lines of FSTL1 were selected with puromycin for 2 weeks. Subsequently, cervical cancer cells were infected with lenti-cas9-puro lentiviral particles, the latter being infected with lentivirus-sgRNA-FSTL1 or lentivirus-sgRNA-NC, respectively. The expression of FSTL1 at the protein level was detected by western blotting.

Screening for active sgRNA. Genomic DNA was extracted by using a nucleic acid extraction kit (cat. no. D3121; Magen Biotechnology Co., Ltd.). Active sgRNA was screened using the KO and mutation detection kit. The PCR reaction was conducted in accordance with the following system to obtain a hybrid DNA product. Briefly, after an initial denaturation step at 95°C for 2 min, amplifications were conducted with 35 cycles at a melting temperature of 95°C for 20 sec and 55°C for 20 sec, followed by an annealing temperature of 72°C for 5 min. Then, 3 µl of hybrid DNA product, 2 µl of detecase buffer, 1 µl of detecase and 4 µl of water were mixed and allowed to react for 20 min at 45°C, to which 2 µl of stop buffer was finally added. The final PCR product was detected by 2% agarose gel electrophoresis. The gel was stained with 0.5 µg/ml ethidium bromide solution for 20 min at room temperature and decolorized with deionized water for 10 min. The gel imaging analysis system (Tanon-2500; Shanghai Tianneng Technology Co., Ltd.) was used to observe and analyze the results. The special primer sequences used for this reaction were as follows: sgRNA-1(KO1) forward, 5'-TATCCATAAC TGCACAAACATTCTC' and reverse, 5'-GGCAAACCCAGC AGGCTCATAAG-3'; sgRNA-2(KO2) forward, 5'-GTATGT TTTAGGAAGAGCTAAGGAG-3' and reverse, 5'-CCATGC TTTAAAAATCAGGAATCTG-3'; sgRNA-3(KO3) forward, 5'-ACATGTAGAGCAGCTGTAATCCTAG-3' and reverse, 5'-TCTGACCCAACCAGCTGCTTCAATT-3'.

Colony formation assay and 3-(4,5-dimethylthiazol-2-y1)-2,5-diphenyltetrazolium bromide (MTT) assay. For the cell colony formation assay, HeLa or SiHa cells (1x10³ cells/well) were seeded into a six-well plate and cultured for 6-10 days. The cells

were then washed twice with PBS and fixed with methanol for 30 min. Subsequently, the cells were stained with 1% crystal violet for 20 min at room temperature (Red Rock Reagent Factory). Finally, the fixed cells were washed twice with PBS for 10 min and enumerated manually under an inverted microscope (Olympus Corporation) when the colony contained ≥50 cells. For the MTT assay, HeLa or SiHa cells (3x10³ cells/well) were seeded and cultured in a 96-well plate for 24, 48, 72, 96 and 120 h. Next, 20 µl of PBS containing 0.5% MTT (5 mg/ml, MilliporeSigma) was added to each well and incubated at 37°C for 4 h. Then, the culture medium was discarded and 150 µl of dimethyl sulfoxide was added to dissolve the formazan crystals. Next, 96-well plates containing cells were vibrated at 37°C for 10 min. Finally, the absorbance of each well was determined at 490 nm wavelength by using a microplate reader (Biotek Synergy H1; Agilent Technologies, Inc.).

Wound-healing assay and Transwell assay. For the wound-healing assay, the experimental cells (3x10⁵ cells/well) were seeded into a culture insert (cat. no. 80209; Ibidi GmbH) and cultured at 37°C for 24 h in a humidified atmosphere of 5% CO_2. After 24 h, a wound was created by removing the culture insert. The cells were carefully washed twice in cold PBS and incubated with RPMI-1640 medium without fetal bovine serum at 37°C for 24 h. The Transwell assay was conducted in a 24-well Boyden chamber (cat. no. 3422; Corning, Inc.). Briefly, 3x10⁴ cells were suspended in a serum-free medium and seeded into the upper chamber. Subsequently, 600 µl of 15% fetal bovine serum was added to the lower chamber. After the cells were cultured at 37°C for 12 h, the invasive cells were fixed with methanol for 30 min and then stained with 1% crystal violet for 20 min. Finally, the invasive cells were counted under a light microscope. For the invasion assay, Matrigel® Basement Membrane Matrix (BD Biosciences) and serum-free medium in the ratio of 1 to 3 were pre-coated to the membrane of upper chambers at 4°C and then placed at 37°C for 4-5 h to solidify. After the cells were cultured at 37°C for 24 h, the invasive cells were fixed with methanol for 30 min and stained with 1% crystal violet for 20 min. Other measurements were the same as for the migration assay.

Flow cytometry. Briefly, 1x10⁵ cells were collected and the apoptotic rate was detected by using the APC Annexin V/PI Apoptosis Detection kit (cat. no. KGA1022; Nanjing KeyGen Biotech Co., Ltd.) following the manufacturer's instructions. The cells were sequentially incubated with Annexin V-APC for 15 min and then with PI for 10 min in the dark. Subsequently, the cells were detected by FACS CantoII (BD Biosciences) and analyzed by Flowjo V10 (FlowJo LLC).

Mouse xenograft models. A total of 72 female BALB/C nude mice (age 4-6 weeks old) were purchased from the Animal Experiment Center of Guangxi Medical University and housed in the specific-pathogen-free (SPF) animal facility under controlled temperature and humidity with alternating 12/12-h light and dark cycles. SPF food and sterile water were provided *ad libitum*. The body weight of the mice ranged from 13.52-18.64 g. The nude mice were randomly assigned to the experimental, negative-control group, and mock groups of 6 nude mice each. Briefly, 2x10⁶ [1x10⁷/l (0.2 ml)] cells were

subcutaneously injected into the corresponding axillary region of nude mice. The size of the tumor was measured using vernier calipers every 3 days and then calculated using the following formula: (volume=0.5x long diameter x short diameter^2). All nude mice were sacrificed by cervical dislocation at 27 days. The animal experiments were approved (approval no. 2201805166) by The Animal Care & Welfare Committee of Guangxi Medical University (Nanning, China).

Gene chip analysis. Gene chip analysis was performed in SiHa cell lines overexpressing FSTL1 when compared with negative controls. The assay and data analyses were performed at the Shanghai GeneChem Co., Ltd. in accordance with the protocols of the Affymetrix Gene Chip system. Total RNA was extracted from the cells using TRIzol reagent (Pufei Biotechnology Co., Ltd.). First, a mixture of poly-a RNA and total RNA was synthesized into first-strand cDNA. Second, first-strand cDNA was further synthesized to second-strand cDNA, as the procedure of gene chip as aforementioned by Shanghai GeneChem Co., Ltd. Then, the second-strand cDNA and IVT were applied to synthesize biotin-labeled aRNA. Finally, the data were obtained through purification, hybridization, dyeing and scanning. The results of the gene chip were analyzed and integrated with the Ingenuity Pathway Analysis (IPA) software 23.0 (Qiagen).

Protein extraction and western blotting. The proteins were extracted using the RIPA buffer (cat. no. P0013C; Beyotime Institute of Biotechnology) containing protease inhibitors (P0100; Beijing Solarbio Science & Technology Co., Ltd.). The protein concentration was determined by using the BCA protein assay kit (cat. no. P001S; Beijing Solarbio Science & Technology Co., Ltd.). Equal amounts of proteins (25 μg) were subjected to 12% sodium dodecyl-sulfate polyacrylamide gel electrophoresis (SDS-PAGE) and then transferred onto PVDF membranes (Beijing Solarbio Science & Technology Co., Ltd.). The membranes were incubated with 5% non-fat milk at room temperature for 1 h. Subsequently, the membranes were incubated with specific primary antibodies against FSTL1 (1:500; cat. no. ab71548; Abcam), IGF-1R (1:500; cat. no. 3027; Cell Signaling Technology, Inc.), PI3K (1:250; cat. no. 4255; Cell Signaling Technology, Inc.), AKT (1:250; cat. no. 9272; Cell Signaling Technology, Inc.), phosphorylated (P-)AKT (1:250; cat. no. 4060; Cell Signaling Technology, Inc.), BCL-2 (1:500; cat. no. ab32503; Abcam), BAX (1:500; cat. no. ab32124; Abcam) and GAPDH (1:1,000; cat. no. 5174; Cell Signaling Technology, Inc.) at 4˚C overnight, followed by incubation with horseradish peroxidase (HRP)-conjugated secondary antibody (1:15,000; cat. no. 7074; Cell Signaling Technology, Inc.) at 37˚C for 2 h. The immunoreactive bands were visualized using the ECL kit (cat. no. P0018; Beijing Solarbio Science & Technology Co., Ltd.) and analyzed using ImageJ software (version 2.1.4.7; National Institutes of Health). The relative expression of the target proteins was normalized to GAPDH.

Statistical analysis. All the data were analyzed using SPSS Statistics V22.0 software (IBM Corp.). The measurement data was tested for normal distribution using the Shapiro-Wilk method. If the data showed a normal distribution, it was expressed as the mean ± standard deviation (SD). The differences between the two groups and among the three groups were analyzed using two-independent sample Student's t-test and one-way analysis of variance (ANOVA), respectively. The least significant difference (LSD) method was applied by following ANOVA. If the data did not conform to a normal distribution, it was expressed as a median (interquartile range). The non-parametric test method was applied for the difference between the groups. Count data was described in relative numbers. The expression of FSTL1 at the mRNA and protein levels was analyzed using the Chi-square test. The mock group was equivalent to a blank control, and nothing was added to the blank group. P≤0.05 was considered to indicate a statistically significant difference (two-tailed).

Results

FSTL1 expression is downregulated at the mRNA and protein levels in cervical cancer tissues. FSTL1 expression at the mRNA and protein levels was detected in cervical cancer tissues using RT-qPCR and IHC, respectively. The findings indicated that the expression of FSTL1 at the mRNA and protein levels was downregulated in cervical cancer tissues compared with tumor-adjacent or normal cervical tissues (P<0.001, Fig. 1A and D). According to the observations, the expression of FSTL1 mRNA was gradually increased in cervical cancer tissues, tumor-adjacent tissues, and normal cervical tissues (P<0.001, Fig. 1A). In addition, the expression of FSTL1 mRNA in the matched cancer tissues was downregulated compared with the tumor-adjacent tissues (P<0.001, Fig. 1B), and that in the non-matching cancer tissues was downregulated compared with the normal cervical tissues (P<0.001, Fig. 1C). FSTL1 protein expression was lower in the cervical cancer tissues compared with that in the normal cervical tissues (P=0.006). Moreover, the expression was predominantly localized in the nucleus, but some expression was also detected in the cytoplasm (Fig. 1D).

FSTL1 expression is associated with the clinical features of patients with cervical cancer. To determine the relationship between FSTL1 expression and clinical features in patients with cervical cancer, the cervical cancer tissues were categorized into high- and low-expression groups based on the median expression of FSTL1 mRNA. The low expression of FSTL1 mRNA was observed to be associated with the infiltration depth (P=0.037) and pathologic type (P=0.05) (Table I). Subsequently, the cervical cancer tissues were classified into high- and low-expression groups based on the median IRS of FSTL1 protein expression. The findings demonstrated that the low expression of FSTL1 at the protein level was linked to the infiltration depth (P=0.021) and degree of differentiation (P=0.002). On the contrary, the expression of FSTL1 at the mRNA and protein levels was not related to age, FIGO stage, or lymph node metastasis (P>0.05) (Table I).

Screening and verification of stable strains of cervical cancer cells with FSTL1 OE or KO. HeLa and SiHa cells were infected with lentivirus-FSTL1 or lentivirus-NC. Stable strains of cervical cancer cells with FSTL1 OE or KO were
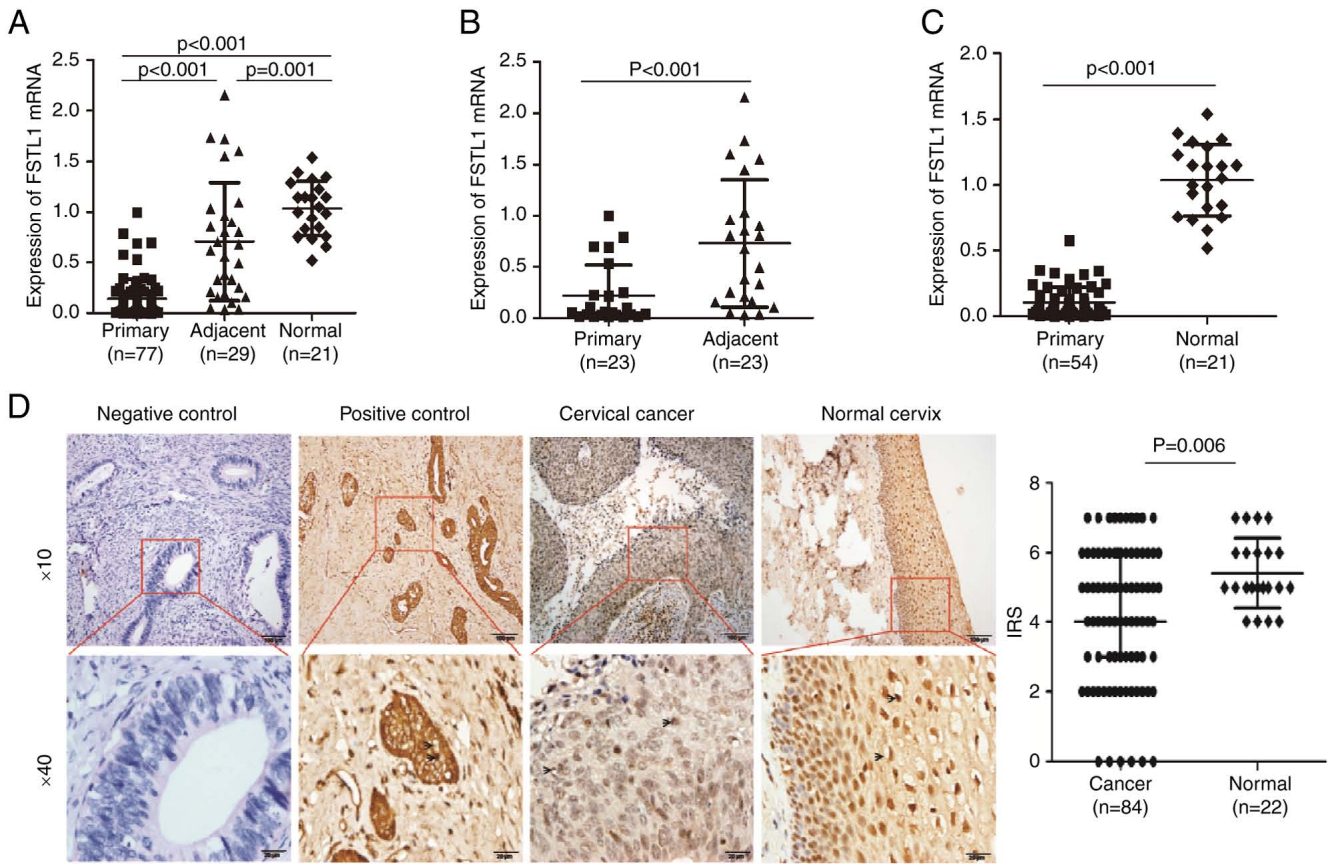
Figure 1. Expression of FSTL1 is downregulated in cervical cancer tissues. (A) The expression of FSTL1 at the mRNA level was downregulated in cervical cancer tissues compared with that in the tumor-adjacent tissues or normal cervical tissues. The expression of FSTL1 at the mRNA level gradually increased in the cervical cancer tissues, tumor-adjacent tissues and normal cervical tissues. (B) The expression of FSTL1 at the mRNA level in the matched cancer tissues was downregulated compared with that in the tumor-adjacent tissues. (C) The expression of FSTL1 at the mRNA level in the non-matching cancer tissues was downregulated compared with that in the normal cervical tissues. (D) The expression of FSTL1 protein was downregulated in the cervical cancer tissues. Prostate cancer tissues served as the positive-control. PBS was replaced with the primary antibody in the negative-control group. A total of 84 cervical cancer tissues and 22 normal cervical tissues were detected by immunohistochemistry. The FSTL1 protein expression was found to be decreased in the cervical cancer tissues compared with that in the normal cervical tissues. FSTL1 protein was mainly localized in the nucleus. Data are expressed as the median (interquartile range) and analyzed by non-parametric test. FSTL1, follistatin-like protein 1.

selected with puromycin for 2 weeks. The fluorescence efficiency of stable strains of cervical cancer cells was observed under a fluorescence microscope, which revealed that the lentiviral infection efficiency of cells with OE or KO of FSTL1 was >80% (Fig. 2A and E). RT-qPCR assay suggested that FSTL1 mRNA expression was upregulated in the OE group compared with the NC and mock (MOCK) groups (Fig. 2B). Western blotting signified that the expression of the FSTL1 protein was upregulated in the OE group compared with the NC and MOCK groups (Fig. 2C and D). Furthermore, RT-qPCR assay demonstrated that the expression of FSTL1 mRNA was downregulated in the KO group compared with the NC and MOCK groups (Fig. 2F). Western blotting assay signified that the expression of the FSTL1 protein was downregulated in the KO group compared with the NC and MOCK groups (Fig. 2I and J). Cruiser TM assay showed that the KO1 and KO3 targets were active, the KO2 target was inactive, and the KO3 target activity was comparatively improved (Fig. 2G). The sequencing of the plasmids containing the three sgRNAs is presented in Fig. 2H. These results indicated that cervical cancer cells with FSTL1 KO or OE were successfully created.

OE of FSTL1 inhibits proliferation, migration and invasion and promotes apoptosis in cervical cancer cells. To comprehend the biological characteristics of FSTL1 *in vitro*, HeLa and SiHa cells were infected with lentivirus-FSTL1 or lentivirus-NC. The results of the MTT assay indicated that the proliferation of both HeLa and SiHa cells was inhibited in the FSTL1 OE group compared with the NC and MOCK groups (Fig. 3A). Moreover, FSTL1 OE significantly inhibited the proliferation of HeLa and SiHa cells on the 3rd and 4th day respectively. Subsequently, the colony formation assay was performed to explore whether FSTL1 affected the single-cell proliferation of HeLa and SiHa cells. The colony formation rate of HeLa and SiHa cells in the OE group was lower than that in the other two control groups (Fig. 3B). Furthermore, the wound-healing assay demonstrated that FSTL1 OE retarded the migration of HeLa and SiHa cells when compared with that in the NC and MOCK groups (Fig. 3C). Furthermore, invasion and migration in Transwell assay confirmed that the number of invasive and migratory cells in the FSTL1 OE group was significantly less than that in the NC and MOCK groups (Fig. 3D and E). Collectively, these data established that FSTL1 inhibited the migration and
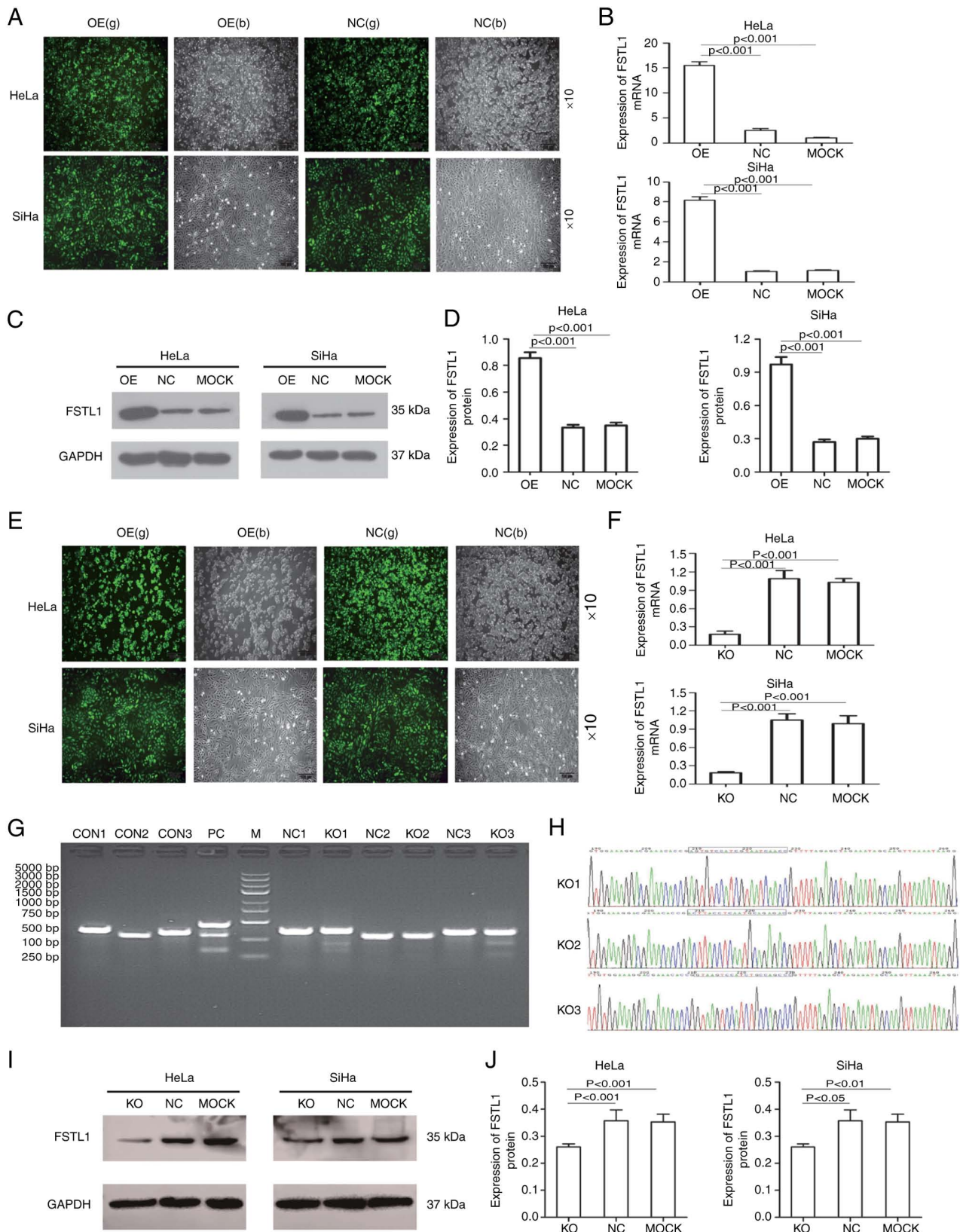
Figure 2. Screening and verification of stable strains of cervical cancer cells overexpressing or knocking out FSTL1. (A and E) The OE or KO of FSTL1 lentiviral infection efficiency was >80% (b: green fluorescence g: bright). (B and F) Reverse transcription-quantitative PCR assay revealed that the expression of FSTL1mRNA was upregulated or downregulated in the FSTL1 OE group or the KO group compared with their corresponding NC group and the mock group (MOCK). (C) Western blotting revealed that the expression of FSTL1 protein was upregulated in the OE group compared with that in their corresponding NC and MOCK groups. (D) Quantified data of panel C. (G) The results of the KO and mutation detection assay revealed that the KO1 and KO3 targets were active, the KO2 target was inactive and the KO3 target activity was improved (M: ladder marker. CON: mock control corresponding to each experimental group. PC: positive-control group). (H) The sequencing of plasmids containing the three sgRNAs. (I) Western blotting revealed that the FSTL1 protein expression was downregulated in the KO groups compared with that in the corresponding NC and MOCK groups. (J) Quantified data of panel I. Data are expressed as the mean ± standard deviation and analyzed by one-way analysis of variance (ANOVA) from three independent experiments. FSTL1, follistatin-like protein 1; OE, overexpression; KO, knockout; NC, negative control; sgRNA, small-guide RNA.
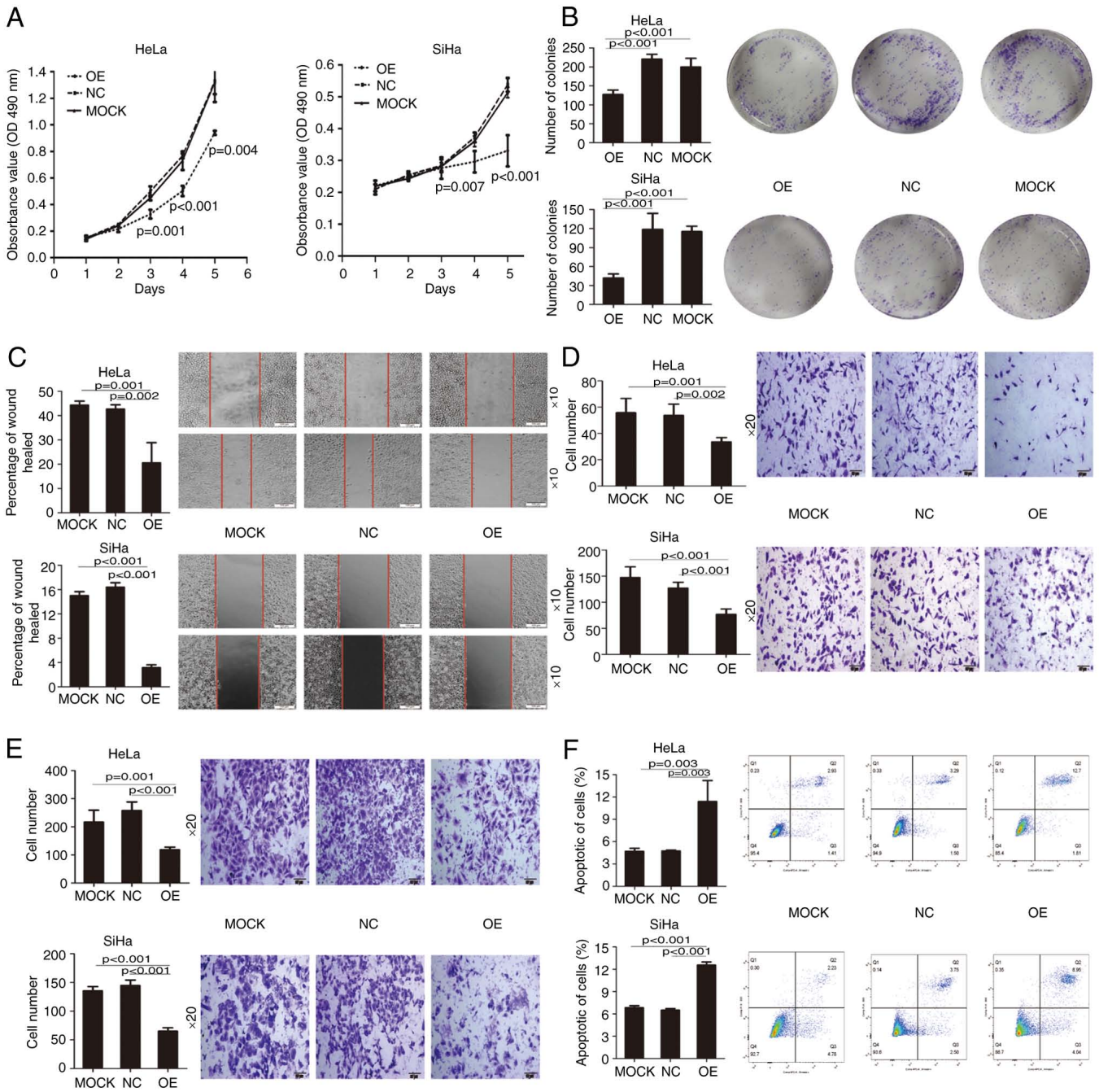
Figure 3. OE of FSTL1 inhibits the proliferation, migration and invasion of cervical cancer cells and promotes cell apoptosis. (A) MTT assay revealed that FSTL1 OE began to significantly inhibit the proliferation of HeLa cells since the 3rd day. However, FSTL1 OE started to significantly inhibit the proliferation of SiHa cells on the 4th day. (B) The colony formation rate of HeLa and SiHa cells in the OE group was significantly lower compared with that in the other two control groups. (C) The wound-healing assay revealed that FSTL1 OE reduced the migration speed of HeLa and SiHa cells compared with the other two control groups. (D and E) The invasion and migration of Transwell assay confirmed that the number of invasive and migratory cells in the FSTL1 OE group was significantly less than that in the other two control groups. (F) Apoptosis assay revealed that the number of apoptotic cells in the FSTL1 OE group was significantly greater than that in the other two control groups. Each experiment was repeated thrice. Data are expressed as the mean ± standard deviation and analyzed by one-way analysis of variance (ANOVA) from three independent experiments. OE, overexpression; FSTL1, follistatin-like protein 1; NC, negative control.

invasion abilities of HeLa and SiHa cells and that it may be a metastasis-related gene in cervical cancer. Finally, the effect of FSTL1 on apoptosis was detected using flow cytometric analysis. Apoptosis assay demonstrated that the number of apoptotic cells in the FSTL1 OE group was significantly higher than that in the NC and MOCK groups (Fig. 3F), which proved that the OE of FSTL1 promoted apoptosis in cervical cancer cells.

KO of FSTL1 promotes proliferation, migration and invasion and inhibits apoptosis in cervical cancer cells. To decipher the effects of FSTL1 depletion on the biological function of cervical cancer cells, HeLa and SiHa cells were infected with lentivirus-Cas9-sgRNA-FSTL1 or lentivirus-Cas9-sgRNA-NC. MTT assay was subsequently performed, which indicated that the proliferation of both HeLa and SiHa cells was promoted in the FTL1 KO group
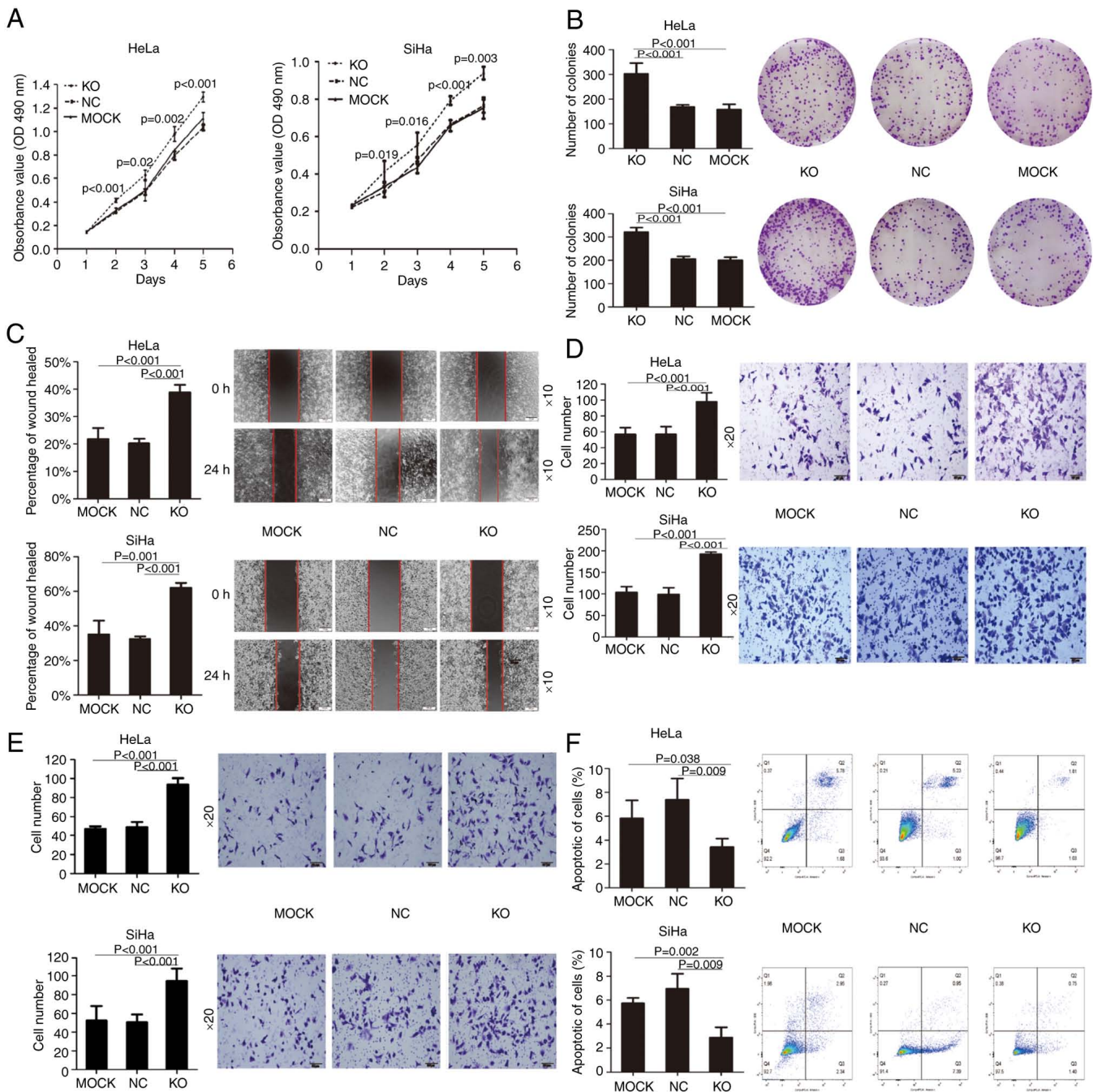
Figure 4. KO of FSTL1 promotes the proliferation, migration and invasion of cervical cancer cells and inhibits cell apoptosis. (A) MTT assay showed that the KO of FSTL1 began to significantly promote the proliferation of HeLa cells since the second day. However, the KO of FSTL1 started to significantly promote the proliferation of SiHa cells on the second day. (B) The colony formation assay indicated that the KO of FSTL1 promoted the single-cell proliferation of HeLa and SiHa cells. (C) The wound-healing assay indicated that FSTL1 accelerated the migration speed of HeLa and SiHa cells. (D and E) Invasion and migration of Transwell assay confirmed that the number of invasive and migratory cells in the FSTL1-KO group was significantly greater than that of the other two control groups. (F) Apoptosis assay revealed that the number of apoptotic cells in the FSTL1-KO group was significantly less than that in the other two control groups. Each experiment was repeated thrice. Data are expressed as the mean ± standard deviation and analyzed by one-way analysis of variance (ANOVA) from three independent experiments. KO, knockout; FSTL1, follistatin-like protein 1; NC, negative control.

compared with the NC and MOCK groups (Fig. 4A). KO of FSTL1 significantly promoted the proliferation of HeLa and SiHa cells from the 2nd day. The colony formation assay revealed that the KO of FSTL1 promoted the single-cell proliferation of HeLa and SiHa cells (Fig. 4B). Furthermore, the results of the wound-healing assay demonstrated that the KO of FSTL1 accelerated the migration of HeLa and SiHa cells compared with the two control groups (Fig. 4C).

Moreover, invasion and migration in the Transwell assay confirmed that the number of invasive and migratory cells in the KO group was significantly higher than that in the two control groups (Fig. 4D and E). Succinctly, these results confirmed that the KO of FSTL1 augmented the migration and invasion abilities of HeLa and SiHa cells. Apoptosis assay further revealed that the number of apoptotic cells in the KO group was significantly less than that in the two
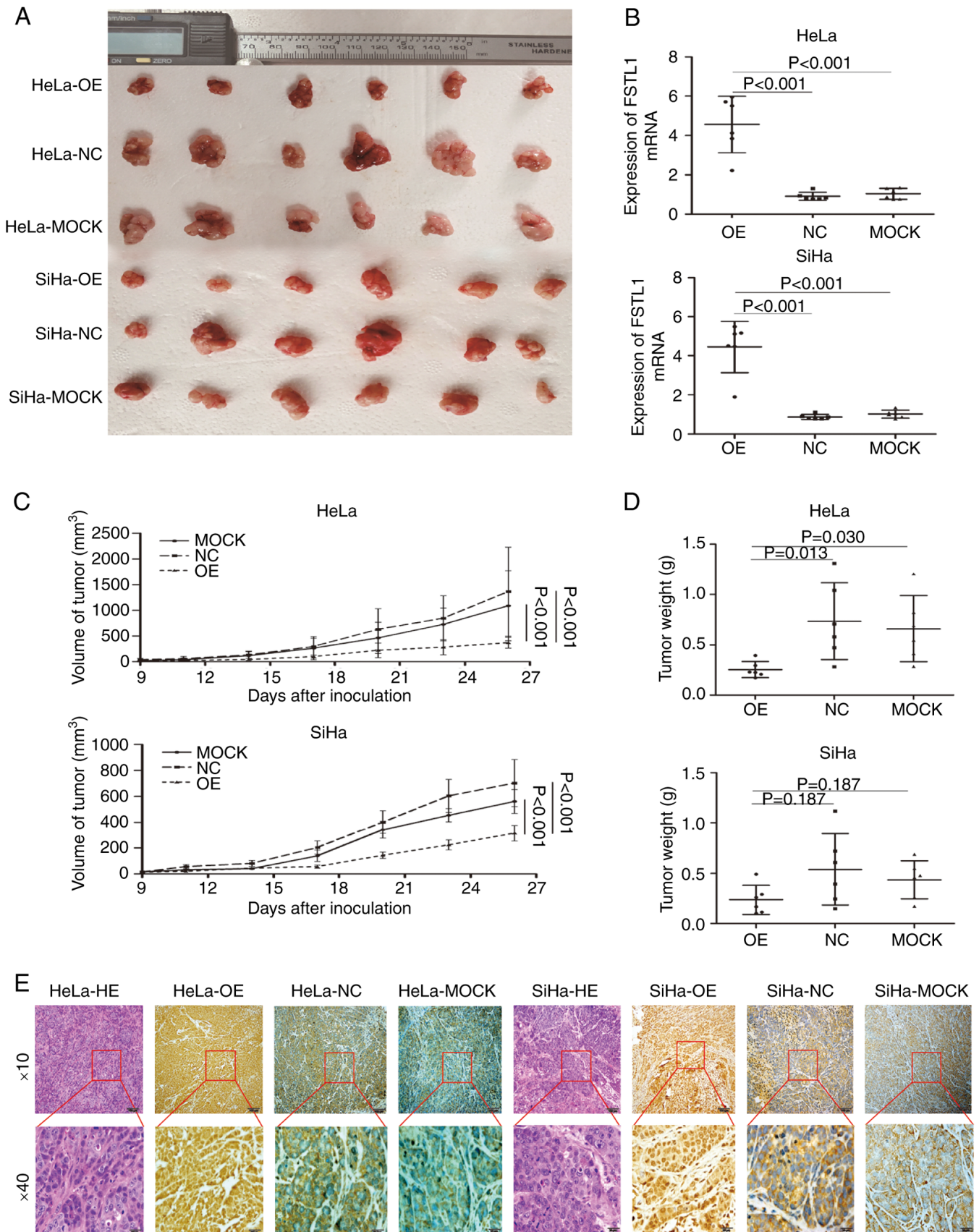
Figure 5. OE of FSTL1 inhibits the growth of xenograft tumors in nude mice. (A) The final volume of tumors in the FSTL1 OE group (n=6) was lower than that in the NC group and the mock group (n=6). (B) The expression of FSTL1 at the mRNA level was significantly higher than that in the other two control groups. (C) The average weight of tumors in the OE group was lower than that in the other two control groups. (D) The growth curve of the tumor was significantly slower in the FSTL1 OE group compared with that in the other two control groups. (E) The images of H&E staining for xenograft tumor tissues and immunohistochemical staining for FSTL1 in the FSTL1 OE, NC and mock groups. Data are expressed as the mean ± standard deviation and analyzed by one-way analysis of variance (ANOVA) from six independent experiments. OE, overexpression; FSTL1, follistatin-like protein 1; NC, negative control.
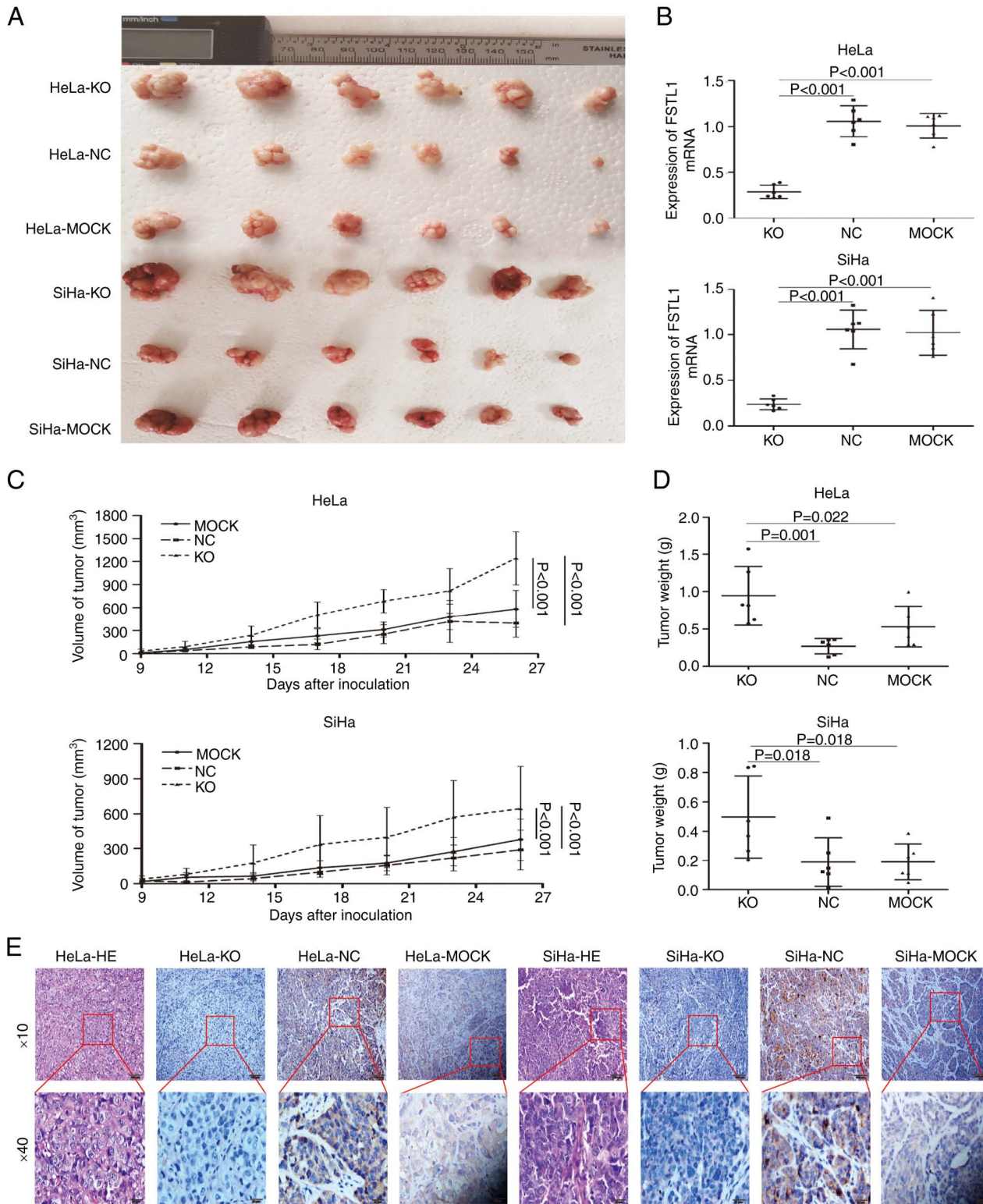
Figure 6. KO of FSTL1 promotes the growth of xenograft tumors with cervical cancer. (A) The final volume of tumors in the FSTL1-depletion group (n=6) was higher than that in the NC group and mock group (n=6). (B) The expression of FSTL1 at the mRNA levels was significantly lower than that in the other two control groups. (C) The average weight of tumors in the FSTL1-depletion group was higher than that in the other two control groups. (D) The growth curve of the tumor in the FSTL1-depletion group was significantly faster than that in the other two control groups. (E) The images of H&E staining for xenograft tumor tissues and immunohistochemical staining for FSTL1 in the FSTL1-depletion group, NC group and mock group. Data are expressed as the mean ± standard deviation and analyzed by one-way analysis of variance (ANOVA) from six independent experiments. KO, knockout; FSTL1, follistatin-like protein 1; NC, negative control.

control groups (Fig. 4F). Collectively, these results confirmed that the KO of FSTL1 inhibited the apoptosis of cervical cancer cells.

FSTL1 inhibits the growth of cervical cancer cell line xenografts. To determine the biological function of FSTL1 *in vivo*, cervical cancer cells overexpressing FSTL1 were
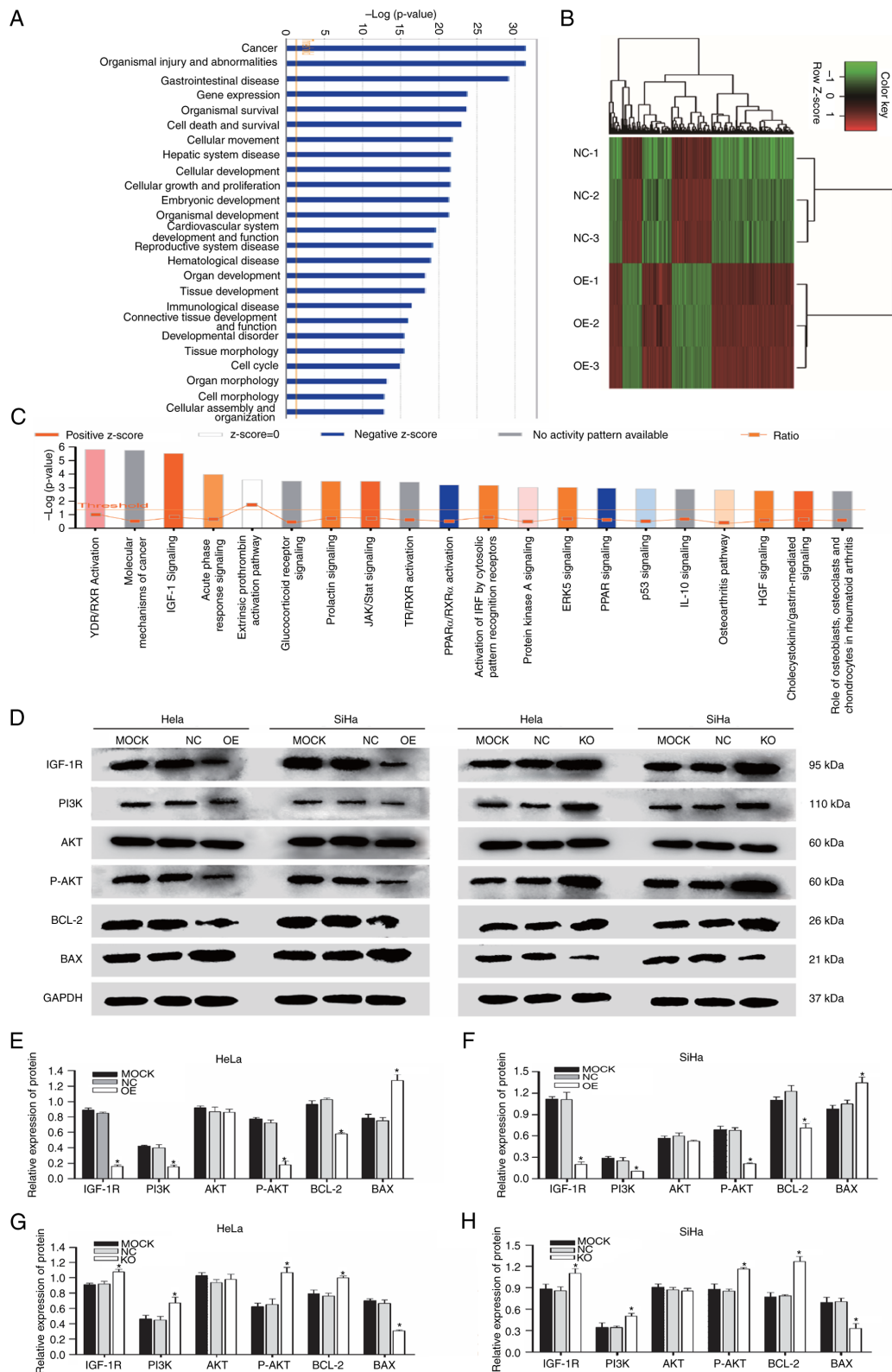
Figure 7. FSTL1 may be involved in the regulation of the IGF-1R/PI3K/AKT/BCL-2 signaling pathway. (A) Disease and functional enrichment analyses revealed that differentially expressed genes of FSTL1 were mainly involved in the regulation of biological processes such as cancer development, damage and development of the body, gastrointestinal diseases and gene expression. (B) Heat map of cluster analysis of upregulated and downregulated differentially expressed genes in HeLa cells (it was based on all genes having been sorted using |Fold change |>2 and FDR <0.05). There were 881 differentially expressed genes in the OE group, of which 593 genes were upregulated and 288 genes were downregulated. (C) Kyoto Encyclopedia of Genes and Genomes and Ingenuity Pathway Analysis signaling pathway enrichment analyses revealed that the differentially expressed genes of FSTL1 were mainly enriched in the cancer transcriptional misregulation signaling, mitogen-activated protein kinase (MAPK) signaling, cancer signaling, P53 signaling and IGF-1 signaling pathways, among which the IGF-1 signaling pathway was significantly activated in this experiment. (D) The IGF-1R, PI3K, AKT, P-AKT, BCL-2 and BAX protein electropherogram. (E-H) The relative protein expression levels of IGF-1R, PI3K, AKT, P-AKT, BCL-2 and BAX in each group. Western blotting revealed that the OE of FSTL1 downregulated IGF-1R, PI3K, AKT, P-AKT and BCL-2, but upregulated BAX. The KO of FSTL1 restored these changes. Data are expressed as the mean ± standard deviation and analyzed by one-way analysis of variance (ANOVA) from three independent experiments. *P<0.05, compared with the control group. FSTL1, follistatin-like protein 1; OE, overexpression; KO, knockout; P-, phosphorylated.

Table II. Top 10 upregulated or downregulated differentially expressed genes in HeLa cells.

Gene symbol	Fold change	P-value	FDR	Regulation
FOS	32.99038	9.83×10^{-18}	3.86×10^{-13}	Up
EGR1	19.41814	1.77×10^{-14}	6.32×10^{-11}	Up
CTGF	12.20367	4.09×10^{-14}	1.15×10^{-10}	Up
PDZD2	10.03935	2.04×10^{-12}	1.29×10^{-9}	Up
ZFP36	9.669648	1.04×10^{-13}	1.95×10^{-10}	Up
ATF3	8.939991	4.71×10^{-11}	9.94×10^{-9}	Up
NR4A1	7.948651	2.0×10^{-15}	2.02×10^{-11}	Up
NR4A2	6.967495	2.26×10^{-13}	2.85×10^{-10}	Up
MALAT1	6.35784	2.51×10^{-11}	6.66×10^{-9}	Up
OASL	5.798434	5.50×10^{-13}	5.03×10^{-10}	Up
DAW1	-23.5035	1.89×10^{-13}	2.66×10^{-10}	Down
GKN2	-19.5982	9.97×10^{-13}	7.63×10^{-10}	Down
CA9	-9.04366	1.62×10^{-12}	1.08×10^{-9}	Down
IL7R	-7.51349	1.02×10^{-10}	1.68×10^{-8}	Down
CDH5	-6.63583	1.04×10^{-10}	1.70×10^{-8}	Down
PTGS1	-6.4919	3.74×10^{-13}	4.06×10^{-10}	Down
CCL20	-6.00781	1.26×10^{-9}	8.09×10^{-8}	Down
LAMA1	-5.99628	1.56×10^{-13}	2.37×10^{-10}	Down
STAMBPL1	-5.8609	9.31×10^{-14}	1.93×10^{-10}	Down
TSNAX-DISC1	-5.83368	1.12×10^{-10}	1.77×10^{-8}	Down

Table III. Top 5 upregulated or downregulated KEGG pathway enrichment analysis of differentially-expressed downstream genes of FSTL1 in HeLa cells.

Gene Ontology ID	Signaling pathway	Database	P-value	Genes	Regulation
hsa05202	Transcriptional misregulation in cancer	KEGG	<0.001	18	Up
hsa04010	MAPK signaling pathway	KEGG	<0.001	21	Up
hsa05200	Pathways in cancer	KEGG	0.003	25	Up
hsa04915	Estrogen signaling pathway	KEGG	0.003	10	Up
hsa04910	Insulin signaling pathway	KEGG	0.01	11	Up
hsa05202	Transcriptional misregulation in cancer	KEGG	0.004	9	Down
hsa05222	Small cell lung cancer	KEGG	0.009	6	Down
hsa04115	p53 signaling pathway	KEGG	0.018	5	Down
hsa05145	Toxoplasmosis	KEGG	0.032	6	Down
hsa03040	Spliceosome	KEGG	0.049	6	Down

KEGG, Kyoto Encyclopedia of Genes and Genomes; FSTL1, follistatin-like protein 1.

subcutaneously injected into the axillary region of nude mice. After 27 days, the average weight and final volume of the tumor in the FSTL1 OE group were significantly lower than those in the NC group (Fig. 5A, C and D). RT-qPCR and IHC assays showed that the expression of FSTL1 at the mRNA and protein levels was significantly higher compared with the NC group (Fig. 5B and E). Moreover, cervical cancer cells with FSTL1 KO were subcutaneously injected into the axillary region of nude mice (Fig. 6A-E). The findings signified that the biological functions of the FSTL1 KO group were opposite to those of the OE group

in vivo. Collectively, FSTL1 could inhibit xenograft tumor growth in nude mice.

FSTL1 possibly regulates the IGF-1R/PI3K/AKT/BCL-2 signaling pathway. To clarify the regulatory mechanism of FSTL1 in cervical cancer, gene chip analysis and bioinformatics methods were used to analyze the interaction and relationship between FSTL1 and its downstream signaling pathways. The results of gene chip analysis suggested that compared with the NC group, 881 differentially expressed genes were present in the OE group, of which 593 were upregulated and 288 were

downregulated (Fig. 7B and Table II). Disease and functional enrichment analysis revealed that the differentially expressed genes were predominantly involved in regulating biological processes including cancer development, damage and development of the body, gastrointestinal diseases and gene expression (Fig. 7A). Furthermore, according to KEGG and IPA signaling pathway enrichment analysis, the differentially expressed genes of FSTL1 were chiefly enriched in cancer transcriptional misregulation, mitogen-activated protein kinase (MAPK), cancer, P53, and IGF-1 signaling pathways, of which the IGF-1 signaling pathway was significantly activated in this experiment (Fig. 7C; Table III). The results of western blotting analysis suggested that FSTL1 OE downregulated IGF-1R, PI3K, P-AKT and BCL-2 but upregulated BAX (Fig. 7D-F). On the contrary, FSTL1 KO restored these changes (Fig. 7D, G and H). These findings indicated that in cervical cancer, FSTL1 may be involved in the regulation of the IGF-1R/PI3K/AKT signaling pathway, thereby leading to the activation of the BCL-2 family.

Discussion

In the present study, the expression of FSTL1 in cervical cancer tissues was detected using RT-qPCR and IHC analyses. These investigations revealed that the expression of FSTL1 mRNA and protein was significantly decreased in cervical cancer tissues compared with the corresponding tumor-adjacent and normal cervical tissues. These findings were consistent with the latest relevant studies, affirming that the FSTL1 expression is reduced in cervical cancer tissues (14). The results also established a gradual increase in the expression of FSTL1 mRNA in cervical cancer, tumor-adjacent and normal cervical tissues. Furthermore, the FSTL1 expression was associated with the clinicopathological features of patients with cervical cancer. Low FSTL1 mRNA expression was observed in association with the extent of tumor differentiation and infiltration depth, whereas low FSTL1 protein expression was associated with the pathological type and infiltration depth. Thus, infiltration depth was associated with both mRNA and protein expression levels. Nonetheless, several discrepancies were observed between the IHC and mRNA expression levels of FSTL1. This difference may be attributed to multiple levels of gene expression regulation, the transcription level regulation being the only one link, and post-transcriptional, translational and post-translational regulations playing a role in the final protein expression. Moreover, factors including mRNA degradation, protein degradation, modification and folding may have contributed to the inconsistency between mRNA abundance and the protein expression (18,19). Next, stable strains of cervical cancer with FSTL1 OE and KO were constructed in HeLa and SiHa cells. Certain functional assays were performed both in vitro and in vivo. The findings demonstrated that FSTL1 OE inhibited the proliferation, migration and invasion of HeLa and SiHa cells and enhanced their apoptosis in vitro. In addition, FSTL1 OE suppressed xenograft tumor growth in nude mice in vivo, whereas inhibition of FSTL1 expression resulted in the opposite effect. These observations support that FSTL1 is a potential new diagnostic marker for

cervical cancer. Therefore, it is feasible to detect the expression of FSTL1 in sample tissues to estimate progression in cervical cancer cases. However, there are several drawbacks to tissue protein detection method, including that it is time-consuming and expensive and the inaccessibility to dynamic contrast and follow-up after lesion resection. The detection of the gene expression in the blood is convenient, economical and highly accepted by patients. This technique can be dynamically compared after treatment and is convenient for follow-up observation. If the expression of FSTL1 mRNA in the blood is correlated with the clinical pathology of cervical cancer patients, the FSTL1 level in the blood of cervical cancer patients could serve as one of the severity indicators to assist in the judging of the progression of cervical cancer. However, FSTL1 expression in the blood was not examined in the present study.

Previous studies have reported that FSTL1 participates in the occurrence of tumors by regulating multiple signaling pathways, such as the NF-kB (6) and BMP/Smad signaling pathways (14). In the present study, it was revealed that several novel signaling pathways regulated by FSTL1 are closely related to the occurrence and development of cervical cancer. The results of gene chip analysis indicated the presence of 881 differentially expressed genes after FSTL1 OE. These genes were chiefly enriched in cancer transcriptional misregulation, MAPK, cancer, P53 and IGF-1 signaling pathways. Of these, the IGF-1 signaling pathway was markedly altered. Previous studies have identified that IGF-1 and its receptor (IGF-1R) are aberrantly expressed in several tumors, stimulating the growth of different types of cells and blocking their apoptosis (20-23). IGF-1 promotes cancer development mainly via the PI3K/AKT (24,25) and Ras/MAPK pathways (26). Disorders related to the PI3K/AKT signaling pathway occur in various human diseases, including cancer (27,28), diabetes (29), cardiovascular (30) and neurological disease (31). In cancer, activated AKT regulates different cellular biological functions in the following ways: i) regulation of cell growth by activating mTOR and downstream molecules (25); ii) regulation of cell proliferation by phosphorylating p27 (32) iii) direct inhibition of cell apoptosis by inhibiting apoptotic proteins (such as BAX) (33) or transcription factors (such as FOXO) (34) iv) participation in cell migration and invasion by regulating E-cadherin and vimentin (35) and v) regulation of NF-κB signaling pathway via phosphorylation of IKK (36). Bcl-2 is one of the key effector molecules downstream of the PI3K/AKT signaling pathway and can inhibit cell apoptosis and lead to various diseases (37). When PI3K-dependent AKT is activated, Bcl-2 is phosphorylated, and free Bcl-2 exerts an antiapoptotic effect (37). Hers et al (38) reported that the PI3K/AKT signaling pathway regulates tumor cells by phosphorylating a range of downstream targets, including Bcl-2 family members and caspase. Yang et al (13) observed that FSTL1 inhibited cell apoptosis in hepatocellular carcinoma by silencing AKT/GSK-3β/Bcl2/BAX/Bim signaling. In the present study, for the first time to the best of our knowledge, it was demonstrated that the OE of FSTL1 downregulated IGF-1R, PI3K, P-AKT and BCL-2 but upregulated BAX. KO of FSTL1 restored these changes. These findings suggest the involvement of FSTL1 in the regulation of the IGF-1R/PI3K/AKT/BCL-2 signaling pathway in cervical cancer.

Collectively, the present study revealed that FSTL1 was downregulated in cervical cancer tissues. FSTL1 inhibited the proliferation, migration and invasion of cervical cancer cells and promoted their apoptosis. Furthermore, FSTL1 inhibited xenograft tumor growth in nude mice. FSTL1 may be involved in the regulation of the IGF-1R/PI3K/AKT/BCL-2 signaling pathway in cervical cancer. Hence, it may be exploited as a novel biomarker to evaluate disease progression in patients with cervical cancer. Prognosis evaluation and treatment in such patients could therefore be improved.

Availability of data and materials

The datasets used and/or analyzed during the current study are available from the corresponding author on reasonable request.

Authors' contributions

ZL, XH and HZ conceived and designed the experiments. ZL and HZ prepared the manuscript. ZL, XH and HZ confirm the authenticity of all the raw data. All authors read and approved the final version of the manuscript.

Ethics approval and consent to participate

The present study complied with the guidelines outlined in the Declaration of Helsinki and was approved (approval no. KY-LW-2017-5) by the Ethics Committee of the People's Hospital of Guangxi Zhuang Autonomous Region (Nanning, China). The animal experiments were approved (approval no. 2201805166) by The Animal Care & Welfare Committee of Guangxi Medical University (Nanning, China). Animal ethics review follows the Guiding Opinions on the Treatment of Laboratory Animals issued by the Ministry of Science and Technology of China and the Laboratory Animal-Guideline for Ethical Review of Animal Welfare issued by the National Standard GB/T35892-2018 of China. Written informed consent was obtained by all patients.

Patient consent for publication

Not applicable.

Competing interests

The authors declare that they have no competing interests.

References

1. Ferlay J, Colombet M, Soerjomataram I, Mathers C, Parkin DM, Piñeros M, Znaor A and Bray F: Estimating the global cancer incidence and mortality in 2018: GLOBOCAN sources and methods. Int J Cancer 144: 1941-1953, 2019.
2. Lei J, Ploner A, Elfström KM, Wang J, Roth A, Fang F, Sundström K, Dillner J and Sparén P: HPV vaccination and the risk of invasive cervical cancer. N Engl J Med 383: 1340-1348, 2020.
3. Di Domenico M, Giovane G, Kouidhi S, Iorio R, Romano M, De Francesco F, Feola A, Siciliano C, Califano L and Giordano A: HPV epigenetic mechanisms related to oropharyngeal and cervix cancers. Cancer Biol Ther 19: 850-857, 2018.
4. Mattiotti A, Prakash S, Barnett P and van den Hoff MJB: Follistatin-like 1 in development and human diseases. Cell Mol Life Sci 75: 2339-2354, 2018.
5. Bradshaw AD: Diverse biological functions of the SPARC family of proteins. Int J Biochem Cell Biol 44: 480-488, 2012.
6. Liu YK, Jia YJ, Liu SH and Ma J: FSTL1 increases cisplatin sensitivity in epithelial ovarian cancer cells by inhibition of NF-κB pathway. Cancer Chemother Pharmacol 87: 405-414, 2021.
7. Ni X, Cao X, Wu Y and Wu J: FSTL1 suppresses tumor cell proliferation, invasion and survival in non-small cell lung cancer. Oncol Rep 39: 13-20, 2018.
8. Liu Y, Han X, Yu Y, Ding Y, Ni C, Liu W, Hou X, Li Z, Hou J, Shen D, et al: A genetic polymorphism affects the risk and prognosis of renal cell carcinoma: Association with follistatin-like protein 1 expression. Sci Rep 6: 26689, 2016.
9. Wang H, Huang S, Wu S, Yin S, Tang A and Wen W: Follistatin-like protein-1 upregulates dendritic cell-based immunity in patients with nasopharyngeal carcinoma. J Interferon Cytokine Res 37: 494-502, 2017.
10. Lau MCC, Ng KY, Wong TL, Tong M, Lee TK, Ming XY, Law S, Lee NP, Cheung AL, Qin YR, et al: FSTL1 promotes metastasis and chemoresistance in esophageal squamous cell carcinoma through NFκB-BMP signaling cross-talk. Cancer Res 77: 5886-5899, 2017.
11. Wu M, Ding Y, Wu N, Jiang J, Huang Y, Zhang F, Wang H, Zhou Q, Yang Y, Zhuo W and Teng L: FSTL1 promotes growth and metastasis in gastric cancer by activating AKT related pathway and predicts poor survival. Am J Cancer Res 11: 712-728, 2021.
12. Su S, Parris AB, Grossman G, Mohler JL, Wang Z and Wilson EM: Up-regulation of follistatin-like 1 by the androgen receptor and melanoma antigen-A11 in prostate cancer. Prostate 77: 505-516, 2017.
13. Yang W, Wu Y, Wang C, Liu Z, Xu M and Zheng X: FSTL1 contributes to tumor progression via attenuating apoptosis in a AKT/GSK-3β-dependent manner in hepatocellular carcinoma. Cancer Biomark 20: 75-85, 2017.
14. Zhao C, Chen Z, Zhu L, Miao Y, Guo J, Yuan Z, Wang P, Li L and Ning W: The BMP inhibitor follistatin-like 1 (FSTL1) suppresses cervical carcinogenesis. Front Oncol 13: 1100045, 2023.
15. Liu W, Gao G, Hu X, Wang Y, Schwarz JK, Chen JJ, Grigsby PW and Wang X: Activation of miR-9 by human papillomavirus in cervical cancer. Oncotarget 5: 11620-11630, 2014.
16. Livak KJ and Schmittgen TD: Analysis of relative gene expression data using real-time quantitative PCR and the 2(-Delta Delta C(T)) method. Methods 25: 402-408, 2001.
17. Wang J, Zhang S, Wu J, Lu Z, Yang J, Wu H, Chen H, Lin B and Cao T: Clinical significance and prognostic value of SOX7 expression in liver and pancreatic carcinoma. Mol Med Rep 16: 499-506, 2017.
18. Battle A, Khan Z, Wang SH, Mitrano A, Ford MJ, Pritchard JK and Gilad Y: Genomic variation. Impact of regulatory variation from RNA to protein. Science 347: 664-667, 2015.
19. Laurent JM, Vogel C, Kwon T, Craig SA, Boutz DR, Huse HK, Nozue K, Walia H, Whiteley M, Ronald PC and Marcotte EM: Protein abundances are more conserved than mRNA abundances across diverse taxa. Proteomics 10: 4209-4212, 2010.
20. Cevenini A, Orrù S, Mancini A, Alfieri A, Buono P and Imperlini E: Molecular signatures of the insulin-like growth factor 1-mediated epithelial-mesenchymal transition in breast, lung and gastric cancers. Int J Mol Sci 19: 2411, 2018.

21. Rigiracciolo DC, Nohata N, Lappano R, Cirillo F, Talia M, Scordamaglia D, Gutkind JS and Maggiolini M: IGF-1/IGF-1R/FAK/YAP transduction signaling prompts growth effects in triple-negative breast cancer (TNBC) cells. Cells 9: 1010, 2020.

22. Laron Z and Werner H: Congenital IGF-1 deficiency protects from cancer: Lessons from Laron syndrome. Endocr Relat Cancer 30: e220394, 2023.

23. Kwon H, Choi M, Ahn Y, Jang D and Pak Y: Flotillin-1 palmitoylation turnover by APT-1 and ZDHHC-19 promotes cervical cancer progression by suppressing IGF-1 receptor desensitization and proteostasis. Cancer Gene Ther 30: 302-312, 2023.

24. Sun L, Yuan W, Wen G, Yu B, Xu F, Gan X, Tang J, Zeng Q, Zhu L, Chen C and Zhang W: Parthenolide inhibits human lung cancer cell growth by modulating the IGF-1R/PI3K/Akt signaling pathway. Oncol Rep 44: 1184-1193, 2020.

25. Wang C, Sun Y, Cong S and Zhang F: Insulin-like growth factor-1 promotes human uterine leiomyoma cell proliferation via PI3K/AKT/mTOR pathway. Cells Tissues Organs 212: 194-202, 2023.

26. Solarek W, Koper M, Lewicki S, Szczylik C and Czarnecka AM: Insulin and insulin-like growth factors act as renal cell cancer intratumoral regulators. J Cell Commun Signal 13: 381-394, 2019.

27. Liu Y, Zheng P, Jiao T, Zhang M, Wu Y, Zhang X, Wang S and Zhao Z: Paiteling induces apoptosis of cervical cancer cells by down-regulation of the E6/E7-Pi3k/Akt pathway: A network pharmacology. J Ethnopharmacol 305: 116062, 2023.

28. Ma Y, Chen X, Ding T, Zhang H, Zhang Q, Dai H, Zhang H, Tang J and Wang X: KAT7 promotes radioresistance through upregulating PI3K/AKT signaling in breast cancer. J Radiat Res 64: 448-456, 2023.

29. Mao YP, Song YM, Pan SW, Li N, Wang WX, Feng BB and Zhang JH: Effect of codonopsis radix and polygonati rhizoma on the regulation of the IRS1/PI3K/AKT signaling pathway in type 2 diabetic mice. Front Endocrinol (Lausanne) 13: 1068555, 2022.

30. Zhou WW, Dai C, Liu WZ, Zhang C, Zhang Y, Yang GS, Guo QH, Li S, Yang HX and Li AY: Gentianella acuta improves TAC-induced cardiac remodelling by regulating the Notch and PI3K/Akt/FOXO1/3 pathways. Biomed Pharmacother 154: 113564, 2022.

31. Tian Q, Guo Y, Feng S, Liu C, He P, Wang J, Han W, Yang C, Zhang Z and Li M: Inhibition of CCR2 attenuates neuroinflammation and neuronal apoptosis after subarachnoid hemorrhage through the PI3K/Akt pathway. J Neuroinflammation 19: 312, 2022.

32. Yoon JH, Shin JW, Pham TH, Choi YJ, Ryu HW, Oh SR, Oh JW and Yoon DY: Methyl lucidone induces apoptosis and G_2/M phase arrest via the PI3K/Akt/NF-κB pathway in ovarian cancer cells. Pharm Biol 58: 51-59, 2020.

33. Tan X, Gong L, Li X, Zhang X, Sun J, Luo X, Wang Q, Chen J, Xie L and Han S: Promethazine inhibits proliferation and promotes apoptosis in colorectal cancer cells by suppressing the PI3K/AKT pathway. Biomed Pharmacother 143: 112174, 2021.

34. Mishra S, Cosentino C, Tamta AK, Khan D, Srinivasan S, Ravi V, Abbotto E, Arathi BP, Kumar S, Jain A, *et al*: Sirtuin 6 inhibition protects against glucocorticoid-induced skeletal muscle atrophy by regulating IGF/PI3K/AKT signaling. Nat Commun 13: 5415, 2022.

35. Chen L, Qing J, Xiao Y, Huang X, Chi Y and Chen Z: TIM-1 promotes proliferation and metastasis, and inhibits apoptosis, in cervical cancer through the PI3K/AKT/p53 pathway. BMC Cancer 22: 370, 2022.

36. Zhang X, Qu P, Zhao H, Zhao T and Cao N: COX-2 promotes epithelial-mesenchymal transition and migration in osteosarcoma MG-63 cells via PI3K/AKT/NF-κB signaling. Mol Med Rep 20: 3811-3819, 2019.

37. Siddiqui WA, Ahad A and Ahsan H: The mystery of BCL2 family: Bcl-2 proteins and apoptosis: An update. Arch Toxicol 89: 289-317, 2015.

38. Hers I, Vincent EE and Tavaré JM: Akt signalling in health and disease. Cell Signal 23: 1515-1527, 2011.